study. These factors together may have obscured the TIMP-1–inducing property of VS in this study.

Clinical Implication

Early short-term VS strategy appears to be clinically feasible in patients with acute MI. Furthermore, this strategy may be both timely and sufficient based on the following evidence. First, upregulation of plasma and myocardial TNF-α as well as myocardial infiltration of neutrophils are mostly confined to within 3 days after MI.[15,37] Meanwhile, the anti-inflammatory effects of VS are long-lasting. In mice, only 30 seconds of VS significantly suppressed TNF-α activation in response to lipopolysaccharide challenge even at 48 hours after VS.[11] Second, pharmacological inhibition of MMP activity for 48 hours after MI preserves the original extracellular matrix, thereby lessens LV remodeling.[18]

Although the present findings suggest clinically useful strategy of VS, several issues remain to be solved before VS can be considered for clinical application in patients with MI. First, it is unclear whether VS is able to provide additional therapeutic benefits to current pharmacological treatments such as renin-angiotensin-aldosterone inhibition or β-blockade, the efficacy of which has been well established in patients with MI.[38] Second, it is unclear whether VS started after reperfusion is also capable of attenuating LV remodeling after MI. Although we started VS during coronary occlusion in this study, initiating VS after coronary reperfusion may simulate a more clinically relevant situation, because prompt reperfusion of occluded coronary artery is given the utmost priority in the management of patients with acute MI. Further studies to solve these problems are clearly required.

VS did not afford any survival benefit in this study, which is inconsistent with previous findings that VS improves acute[7] or chronic[3] survival in rats after MI by preventing malignant arrhythmia and heart failure. However, the mortality rate in MI rats was ~60% within the first 24 hours in the previous study,[3] which is undoubtedly higher than that seen in MI rabbits of this study (~30%). Low mortality rate in MI rabbits may have masked the impact of VS on survival in this study.

Limitation

We focused on the antiremodeling effects of VS but did not include a detailed mechanistic investigation into how VS reduces LV infarct size. Inflammatory responses to MI play a significant role in determining the infarct size.[9] On the other hand, the infarct size, which reflects the degree of myocardial necrosis, is also one of the determinants of post-MI inflammatory reactions. Therefore, direct cardiomyocyte protection of VS possibly through the muscarinic acetylcholine pathway and the anti-inflammatory effect possibly through the nicotinic pathway may have contributed synergistically to the infarct size-reducing effect of VS. Selective inhibition of the muscarinic and nicotinic pathway by atropine and methyllycaconitine,[39] respectively, may allow elucidation of how these different mechanisms contribute to the beneficial effects of VS in a reperfused MI model. Further studies on these issues are clearly required.

Acute surgical trauma associated with open-chest preparation may have exaggerated the expression of CRP and TNF-α in MI and MI-VS rabbits in this study. For a more rational comparison of acute inflammatory reactions among NC, MI, and MI-VS animals, use of sham-operated rabbits as NC would be more appropriate. Closed-chest animal models of myocardial ischemia-reperfusion[40] may be an alternative to eliminate acute surgical trauma and allow assessment of inflammation strictly from myocardial injury. In this study, MI and MI-VS rabbits underwent identical surgical preparation. Therefore, it is fair to say that the difference in TNF-α expression in infarcts between the MI and MI-VS groups was valid in the present study.

In conclusion, early short-term VS attenuated cardiac dysfunction and myocardial structural remodeling in a rabbit model of reperfused MI. The beneficial effects of VS were associated with suppression of excessive TNF-α activation and myocardial infiltrations of neutrophils.

Acknowledgments

We thank Dr. Takeshi Aiba for his helpful comments on this manuscript.

Disclosures

Supported by Grant-in-Aid for Scientific Research from the Ministry of Education, Culture, Sports, Science and Technology (C-20500404 to K.U.), by a research grant from Nakatani Foundation of Electronic Measuring Technology Advancement (to K.U.), and by Health and Labour Sciences Research Grants from the Ministry of Health, Labour and Welfare of Japan (H19-nano-ippan-009 to M.S.).

References

1. Bolognese L, Cerisano G. Early predictors of left ventricular remodeling after acute myocardial infarction. Am Heart J 1999;138:S79–83.
2. Ezekowitz JA, Kaul P, Bakal JA, Armstrong PW, Welsh RC, McAlister FA. Declining in-hospital mortality and increasing heart failure incidence in elderly patients with first myocardial infarction. J Am Coll Cardiol 2009;53:13–20.
3. Li M, Zheng C, Sato T, Kawada T, Sugimachi M, Sunagawa K. Vagal nerve stimulation markedly improves long-term survival after chronic heart failure in rats. Circulation 2004;109:120–4.
4. Schwartz PJ, De Ferrari GM, Sanzo A, Landolina M, Rordorf R, Raineri C, et al. Long term vagal stimulation in patients with advanced heart failure: first experience in man. Eur J Heart Fail 2008;10:884–91.
5. Katare RG, Ando M, Kakinuma Y, Arikawa M, Handa T, Yamasaki F, et al. Vagal nerve stimulation prevents reperfusion injury through inhibition of opening of mitochondrial permeability transition pore independent of the bradycardiac effect. J Thorac Cardiovasc Surg 2009; 137:223–31.

6. Kawada T, Yamazaki T, Akiyama T, Kitagawa H, Shimizu S, Mizuno M, et al. Vagal stimulation suppresses ischemia-induced myocardial interstitial myoglobin release. Life Sci 2008;83:490–5.
7. Mioni C, Bazzani C, Giuliani D, Altavilla D, Leone S, Ferrari A, et al. Activation of an efferent cholinergic pathway produces strong protection against myocardial ischemia/reperfusion injury in rats. Crit Care Med 2005;33:2621–8.
8. Sun M, Dawood F, Wen WH, Chen M, Dixon I, Kirshenbaum LA, et al. Excessive tumor necrosis factor activation after infarction contributes to susceptibility of myocardial rupture and left ventricular dysfunction. Circulation 2004;110:3221–8.
9. Vinten-Johansen J. Involvement of neutrophils in the pathogenesis of lethal myocardial reperfusion injury. Cardiovasc Res 2004;61: 481–97.
10. Borovikova LV, Ivanova S, Zhang M, Yang H, Botchkina GI, Watkins LR, et al. Vagus nerve stimulation attenuates the systemic inflammatory response to endotoxin. Nature 2000;405:458–62.
11. Huston JM, Gallowitsch-Puerta M, Ochani M, Ochani K, Yuan R, Rosas-Ballina M, et al. Transcutaneous vagus nerve stimulation reduces serum high mobility group box 1 levels and improves survival in murine sepsis. Crit Care Med 2007;35:2762–8.
12. Uemura K, Li M, Tsutsumi T, Yamazaki T, Kawada T, Kamiya A, et al. Efferent vagal nerve stimulation induces tissue inhibitor of metalloproteinase-1 in myocardial ischemia-reperfusion injury in rabbit. Am J Physiol Heart Circ Physiol 2007;293:H2254–61.
13. LaCroix C, Freeling J, Giles A, Wess J, Li YF. Deficiency of M2 muscarinic acetylcholine receptors increases susceptibility of ventricular function to chronic adrenergic stress. Am J Physiol Heart Circ Physiol 2008;294:H810–20.
14. Hasdemir C, Scherlag BJ, Yamanashi WS, Lazzara R, Jackman WM. Endovascular stimulation of autonomic neural elements in the superior vena cava using a flexible loop catheter. Jpn Heart J 2003;44: 417–27.
15. Dewald O, Ren G, Duerr GD, Zoerlein M, Klemm C, Gersch C, et al. Of mice and dogs: species-specific differences in the inflammatory response following myocardial infarction. Am J Pathol 2004;164:665–77.
16. Gwechenberger M, Mendoza LH, Youker KA, Frangogiannis NG, Smith CW, Michael LH, et al. Cardiac myocytes produce interleukin-6 in culture and in viable border zone of reperfused infarctions. Circulation 1999;99:546–51.
17. Klotz S, Foronjy RF, Dickstein ML, Gu A, Garrelds IM, Danser AH, et al. Mechanical unloading during left ventricular assist device support increases left ventricular collagen cross-linking and myocardial stiffness. Circulation 2005;112:364–74.
18. Villarreal FJ, Griffin M, Omens J, Dillmann W, Nguyen J, Covell J. Early short-term treatment with doxycycline modulates postinfarction left ventricular remodeling. Circulation 2003;108:1487–92.
19. Newman KM, Ogata Y, Malon AM, Irizarry E, Gandhi RH, Nagase H, et al. Identification of matrix metalloproteinases 3 (stromelysin-1) and 9 (gelatinase B) in abdominal aortic aneurysm. Arterioscler Thromb 1994;14:1315–20.
20. Emens I, Rouy D, Velot E, Devaux Y, Wagner DR. Adenosine inhibits matrix metalloproteinase-9 secretion by neutrophils: implication of A2a receptor and cAMP/PKA/Ca2+ pathway. Circ Res 2006;99: 590–7.
21. Ørn S, Manhenke C, Anand IS, Squire I, Nagel E, Edvardsen T, et al. Effect of left ventricular scar size, location, and transmurality on left ventricular remodeling with healed myocardial infarction. Am J Cardiol 2007;99:1109–14.
22. Kakinuma Y, Ando M, Kuwabara M, Katare RG, Okudela K, Kobayashi M, et al. Acetylcholine from vagal stimulation protects cardiomyocytes against ischemia and hypoxia involving additive nonhypoxic induction of HIF-1alpha. FEBS Lett 2005;579:2111–8.
23. Frangogiannis NG, Lindsey ML, Michael LH, Youker KA, Bressler RB, Mendoza LH, et al. Resident cardiac mast cells degranulate and release preformed TNF-alpha, initiating the cytokine cascade in experimental canine myocardial ischemia/reperfusion. Circulation 1998;98:699–710.
24. Kindt F, Wiegand S, Niemeier V, Kupfer J, Löser C, Nilles M, et al. Reduced expression of nicotinic alpha subunits 3, 7, 9 and 10 in lesional and nonlesional atopic dermatitis skin but enhanced expression of alpha subunits 3 and 5 in mast cells. Br J Dermatol 2008;159: 847–57.
25. Smart N, Mojet MH, Latchman DS, Marber MS, Duchen MR, Heads RJ. IL-6 induces PI 3-kinase and nitric oxide-dependent protection and preserves mitochondrial function in cardiomyocytes. Cardiovasc Res 2006;69:164–77.
26. Rakhit RD, Seiler C, Wustmann K, Zbinden S, Windecker S, Meier B, et al. Tumour necrosis factor-alpha and interleukin-6 release during primary percutaneous coronary intervention for acute myocardial infarction is related to coronary collateral flow. Coron Artery Dis 2005;16:147–52.
27. Buck JD, Warltier DC, Hardman HF, Gross GJ. Effects of sotalol and vagal stimulation on ischemic myocardial blood flow distribution in the canine heart. J Pharmacol Exp Ther 1981;216:347–51.
28. Ørn S, Manhenke C, Ueland T, Damås JK, Mollnes TE, Edvardsen T, et al. C-reactive protein, infarct size, microvascular obstruction, and left-ventricular remodelling following acute myocardial infarction. Eur Heart J 2009;30:1180–6.
29. Nijmeijer R, Lagrand WK, Lubbers YT, Visser CA, Meijer CJ, Niessen HW, et al. C-reactive protein activates complement in infarcted human myocardium. Am J Pathol 2003;163:269–75.
30. Sukhija R, Fahdi I, Garza L, Fink L, Scott M, Aude W, et al. Inflammatory markers, angiographic severity of coronary artery disease, and patient outcome. Am J Cardiol 2007;99:879–84.
31. Blankenberg S, McQueen MJ, Smieja M, Pogue J, Balion C, Lonn E, et al. Comparative impact of multiple biomarkers and N-Terminal pro-brain natriuretic peptide in the context of conventional risk factors for the prediction of recurrent cardiovascular events in the Heart Outcomes Prevention Evaluation (HOPE) Study. Circulation 2006;114: 201–8.
32. Kelly D, Cockerill G, Ng LL, Thompson M, Khan S, Samani NJ, et al. Plasma matrix metalloproteinase-9 and left ventricular remodelling after acute myocardial infarction in man: a prospective cohort study. Eur Heart J 2007;28:711–8.
33. Lindsey ML, Gannon J, Aikawa M, Schoen FJ, Rabkin E, Lopresti-Morrow L, et al. Selective matrix metalloproteinase inhibition reduces left ventricular remodeling but does not inhibit angiogenesis after myocardial infarction. Circulation 2002;105:753–8.
34. Spinale FG, Escobar GP, Hendrick JW, Clark LL, Camens SS, Mingoia JP, et al. Chronic matrix metalloproteinase inhibition following myocardial infarction in mice: differential effects on short and long-term survival. J Pharmacol Exp Ther 2006;318:966–73.
35. van den Borne SW, Cleutjens JP, Hanemaaijer R, Creemers EE, Smits JF, Daemen MJ, et al. Increased matrix metalloproteinase-8 and -9 activity in patients with infarct rupture after myocardial infarction. Cardiovasc Pathol 2009;18:37–43.
36. Lindsey ML, Escobar GP, Mukherjee R, Goshorn DK, Sheats NJ, Bruce JA, et al. Matrix metalloproteinase-7 affects connexin-43 levels, electrical conduction, and survival after myocardial infarction. Circulation 2006;113:2919–28.
37. Li D, Zhao L, Liu M, Du X, Ding W, Zhang J, et al. Kinetics of tumor necrosis factor alpha in plasma and the cardioprotective effect of a monoclonal antibody to tumor necrosis factor alpha in acute myocardial infarction. Am Heart J 1999;137:1145–52.
38. Landmesser U, Wollert KC, Drexler H. Potential novel pharmacological therapies for myocardial remodelling. Cardiovasc Res 2009;81: 519–27.
39. Liu C, Shen FM, Le YY, Kong Y, Liu X, Cai GJ, Chen AF, Su DF. Antishock effect of anisodamine involves a novel pathway for activating alpha7 nicotinic acetylcholine receptor. Crit Care Med 2009;37: 634–41.
40. Nossuli TO, Lakshminarayanan V, Baumgarten G, Taffet GE, Ballantyne CM, Michael LH, et al. A chronic mouse model of myocardial ischemia-reperfusion: essential in cytokine studies. Am J Physiol Heart Circ Physiol 2000;278:H1049–55.

J Physiol Sci (2010) 60:407–413
DOI 10.1007/s12576-010-0109-8

ORIGINAL PAPER

Both skeletonized and pedicled internal thoracic arteries supply adequate graft flow after coronary artery bypass grafting even during intense sympathoexcitation

Dai Une · Shuji Shimizu · Atsunori Kamiya · Toru Kawada · Toshiaki Shishido · Masaru Sugimachi

Received: 21 February 2010 / Accepted: 15 August 2010 / Published online: 14 September 2010

Abstract The internal thoracic artery (ITA) is harvested by either the pedicled or the skeletonized technique in coronary artery bypass grafting (CABG), with no clear advantage of one technique over the other. We compared graft flow between the pedicled and skeletonized ITA grafts while varying myocardial oxygen demand. CABG was performed to the left anterior descending artery in five anesthetized dogs using a pedicled ITA graft and the graft was subsequently skeletonized. Graft flow was measured during stepwise electrical stimulation of the stellate ganglion. The baseline graft flow before sympathetic stimulation was higher in skeletonized (27.8 ± 1.9 ml/min) than that in pedicled ITA grafts (22.6 ± 2.7 ml/min) ($P < 0.05$). In both ITA grafts, however, graft flow increased to a similar level during sympathetic stimulation that doubled the double product, correlating with the double product. Based on these results, we conclude that metabolic demand can override the potential difference in sympathetic vasoconstriction in both pedicled and skeletonized ITA grafts.

Keywords Coronary artery bypass grafting · Graft flow · Internal thoracic artery · Pedicled · Skeletonized · Sympathetic activation

D. Une · S. Shimizu (✉) · A. Kamiya · T. Kawada · T. Shishido · M. Sugimachi
Department of Cardiovascular Dynamics, National Cerebral and Cardiovascular Center Research Institute, 5-7-1 Fujishiro-dai, Suita, Osaka 565-8565, Japan
e-mail: shujismz@ri.ncvc.go.jp

S. Shimizu
Japan Association for the Advancement of Medical Equipment, Tokyo, Japan

Introduction

The internal thoracic artery (ITA) is the gold standard conduit for coronary artery bypass grafting (CABG) because of its long-term patency [1]. The ITA is harvested by either the pedicled or the skeletonized technique, and which of these two techniques is the better option has been the subject of an extended debate—with as yet no clear conclusion being drawn. Although some human studies [2–4] have demonstrated higher free (pre-anastomosis) flow through skeletonized grafts (with or without topical papaverine), suggesting that the loss of sympathetic nerve-mediated graft vasoconstriction confers an advantage, perfusion pressure was not controlled in these studies. In one study [5] in which the perfusion pressure was controlled, free flow even tended to be lower in skeletonized grafts prior to the administration of intravenous papaverine. Onorati et al. [6] found that graft flows were comparable between the two techniques in the absence of intraluminal papaverine, while Takami and Ina [7], in a comparison of the flow through the anastomosed graft, found that flow was higher through the skeletonized graft.

Flow in the anastomosed graft is likely to be largely dependent on myocardial oxygen demand, suggesting the importance of comparing the flow between the pedicled and skeletonized ITA grafts under varying conditions of myocardial oxygen demand. If the skeletonization procedure were to result in an increased flow capacity, surgeons may be able to perform additional anastomoses to other vessels using the skeletonized ITA, thereby making the skeletonized ITA procedure even more advantageous. If the skeletonization procedure were not able to increase flow capacity, the skeletonized ITA would not be recommended for additional use due to a higher flow reserve. We hypothesized that the skeletonized ITA would have larger

flow capacity due to the loss of sympathetic nerve-mediated graft vasoconstriction.

Materials and methods

Animal preparation

Animal care was provided in accordance with the *Guiding Principles for the Care and Use of Animals in the Field of Physiological Sciences* approved by the Physiological Society of Japan. All protocols were approved by the Animal Subject Committee of the National Cerebral and Cardiovascular Center. Five adult mongrel dogs (weighing 24–35 kg) were anesthetized with intravenous pentobarbital sodium (25 mg/kg) and intubated endotracheally for artificial ventilation with isoflurane and 100% O_2. After a median sternotomy, the heart was suspended in a pericardial cradle. To measure systemic arterial pressure, we placed a fluid-filled catheter in the left subclavian artery via the left brachial artery and connected it to a pressure transducer (DX-200; Nihon Kohden, Tokyo, Japan). The junction of the inferior vena cava and the right atrium was taken as the reference point for zero pressure. An ultrasonic flowmeter (20A594; Transonic Systems, Itaca, NY) was placed around the ascending aorta to measure cardiac output. Electrocardiography leads were also placed for the monitoring electrocardiogram. A catheter was inserted into the femoral vein for fluid replacement (1 ml/kg/h of Ringer's solution). All protocols were performed under open chest conditions.

Pedicled ITA grafting

The left internal thoracic artery (LITA), together with the surrounding veins, muscle, and fascia, was harvested as a pedicled graft using electrocautery. The LITA was harvested from the bifurcation of the musculo-phrenic and superior epigastric arteries up to the upper margin of the first rib or higher. All intercostal branches of the LITA were ligated. After systemic heparinization, the LITA was clamped, and the distal end of the LITA was cut and anastomosed to the left anterior descending artery (LAD). The same surgeon (D.U.) performed the LITA–LAD anastomosis without cardiopulmonary bypass. The heart and the LAD were stabilized using a compression-type mechanical stabilizer (Mini-CABG system; United States Surgical Corporation, Norwalk, CT). A shunt tube was inserted into the LAD to prevent myocardial ischemia during anastomosis. The anastomosis was placed in the mid-LAD [8]. The anastomosis was created using a continuous 7-0 polypropylene suture. The proximal LAD was first ligated after the LITA–LAD anastomosis, and then the LITA was declamped. An angiography was performed after the anastomosis to confirm the absence of stenosis or spasm in the LITA–LAD anastomosis. The LITA graft was sprayed with dilute papaverine (4 mg/ml) to prevent spasm. An ultrasonic flowmeter (2.5S261; Transonic Systems) was placed around the LITA just proximal to the anastomosis. The left stellate ganglion was carefully exposed through a median sternotomy, and a pair of platinum electrodes was attached to it without decentralization. The nerve and electrodes were covered with a mixture of silicone gel (Kwik-Sil; World Precision Instrument, Sarasota, FL). Protocol 1, described below, was carried out following the pedicled LITA grafting.

Skeletonized ITA grafting

Following the completion of protocol 1, the tissue surrounding the graft (including fascia and lymphatics) was stripped up to the most proximal part of the LITA graft in order to skeletonize the LITA graft. The side branches of the LITA were ligated. Fat tissue around the graft was removed as completely as possible based on macroscopic inspection. The adventitia was left as the outermost layer of the graft. The graft was not touched directly with forceps. The graft was sprayed with dilute papaverine (4 mg/ml). After skeletonizing the LITA graft, protocol 2 followed.

Experimental protocols

Since skeletonization always followed pedicled harvesting, protocol 1 (pedicled LITA graft flow measurement) was performed before protocol 2 (skeletonized LITA graft flow measurement) in all dogs. The stimulation of the left sympathetic stellate ganglion for adjusting the voltage amplitude was performed at least 30 min before protocol 1 was initiated.

Protocol 1

The left sympathetic stellate ganglion was electrically stimulated at least 30 min after the completion of the experimental preparation of the pedicled LITA grafts. The frequency of stimulation was increased stepwise from 0 to 10 Hz with increments of 2 Hz. Each step was maintained for 60 s. The pulse duration of the stimulus was set at 5 ms. The voltage amplitude of stimulation (2–5 V) was adjusted in each animal to yield an increase in arterial pressure of approximately 30 mmHg with 10 Hz stimulation. Graft flow, arterial pressure, and cardiac output were recorded for 7 min, which included a 2-min baseline and 5 min of stimulation. These data were sampled at 200 Hz using a 12-bit analog-to-digital converter [AD12-16U(PCI)E;

CONTEC, Osaka, Japan] and stored on the hard disk of a dedicated laboratory computer system.

Protocol 2

At least 30 min after the completion of the experimental preparation of the skeletonized LITA grafts, the left sympathetic stellate ganglion was electrically stimulated in a similar fashion to protocol 1, while all variables were recorded and stored.

Data analysis

Heart rate was calculated from the arterial pressure waveform. Myocardial oxygen demand was estimated as double product (pressure–rate product) and calculated as the product of systolic arterial pressure and heart rate [9]. All variables were averaged during the last 20 s of each electrical stimulation level.

Statistical analysis

All data are presented as the mean ± standard error (SE). In each protocol, one-way repeated measures analysis of variance (ANOVA) followed by Dunnett's test was used to compare variables at each stimulation against the baseline value. The paired t test was used to compare variables between pedicled and skeletonized LITA grafts at each stimulation level. Linear regression analysis was used to examine the relationship between the double product and graft flow. Differences were considered to be significant at a threshold of $P < 0.05$.

Results

Prior to sympathetic stimulation, baseline graft flow (under spontaneous sympathetic outflow) was greater in skeletonized ITA than pedicled ITA (Table 1). Other hemodynamic parameters, including heart rate, cardiac output, mean arterial pressure, and double product, did not differ significantly regardless of harvesting technique.

Table 1 Hemodynamic parameters and graft flow before stimulation

Hemodynamic parameters	Pedicled	Skeletonized	P value
Heart rate (beats/min)	104 ± 8	106 ± 8	NS
Mean arterial pressure (mmHg)	94 ± 7	93 ± 7	NS
Cardiac output (ml/min/kg)	83 ± 17	74 ± 9	NS
Double product (mmHg beats/min)	11368 ± 834	11346 ± 621	NS
Graft flow before stimulation (ml/min)	22.6 ± 2.7	27.8 ± 1.9	<0.05

Values are given as the mean ± standard error (SE)

NS Not significant

Graft flow patterns at baseline and under sympathetic stimulation are shown in Fig. 1a. Sympathetic stimulation increased graft flow ($P < 0.05$) similarly in skeletonized and pedicled ITA grafts, and maximal flow was comparable to each other at 10-Hz stimulation [nonsignificant (NS) difference] (Fig. 1b). Increases in systemic arterial pressure and heart rate did not differ significantly between the two techniques (Fig. 2), and increases in myocardial oxygen demand in response to sympathetic stimulation, as estimated by double product, were likewise similar.

Graft flow (y) correlated well with the double product (x) in both pedicled ($y = 2.6 \times 10^{-3}x - 8.4$, $R^2 = 0.73$) and skeletonized ITA ($y = 2.3 \times 10^{-3}x - 0.7$, $R^2 = 0.69$). The slope and y-intercept did not differ statistically between the two techniques (Fig. 3).

Discussion

The choice of either skeletonized or pedicled ITA grafts for CABG may be an important decision from both the technical and clinical viewpoints; however, clear evidence demonstrating the advantage of either method over the other is not yet available. In this study, we have shown that graft flow increased to a similar level during maximal sympathetic stimulation in both pedicled and skeletonized ITA grafts. These results do not support our hypothesis that the skeletonized ITA would provide larger flow capacity and indicate that coronary vasodilatation in response to increased myocardial oxygen demand is a stronger determinant of graft flow than any possible increase in the vascular resistance of ITA itself. Our study also demonstrates that both skeletonized and pedicled ITAs were able to supply adequate graft flow after CABG even during intense sympathoexcitation.

There are several possible explanations for the difference in graft flow under baseline conditions. First, a loss of sympathetic innervation in the skeletonized graft may have dilated the ITA relative to the pedicled graft under baseline conditions. In support of this explanation, Takami et al. [7] reported that the diameter of the ITA just proximal to the anastomosis is significantly larger in the skeletonized ITA than that in the pedicled ITA. Dönmez et al. [10] reported that the diameter of ITA becomes statically larger by the stellate ganglion blockade. In a preliminary study, we observed that electrical stimulation of the stellate ganglion decreased ITA flow before harvest. Therefore, vasoconstriction may occur in the pedicled ITA during sympathetic stimulation. However, in this study we did not perform simultaneous measurements of the graft flow and diameter

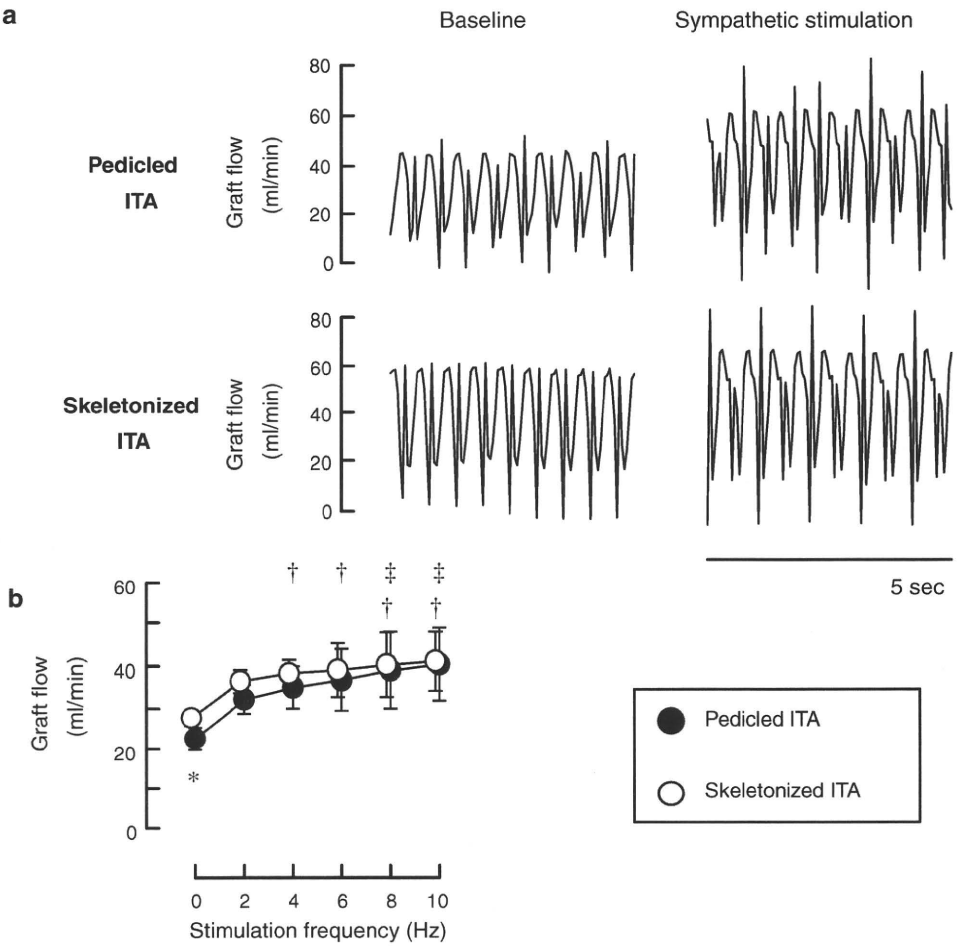

Fig. 1 **a** Typical representative recording of graft flow with pedicled and skeletonized internal thoracic arteries (*ITAs*) during sympathetic nerve stimulation. **b** Mean graft flow with pedicled (*closed circle*) and skeletonized (*open circle*) ITAs during sympathetic nerve stimulation. Data are shown as the mean ± standard error (SE). $^{\dagger}P < 0.05$ vs. baseline, $^{\ddagger}P < 0.01$ vs. baseline, $^{*}P < 0.05$ pedicled vs. skeletonized

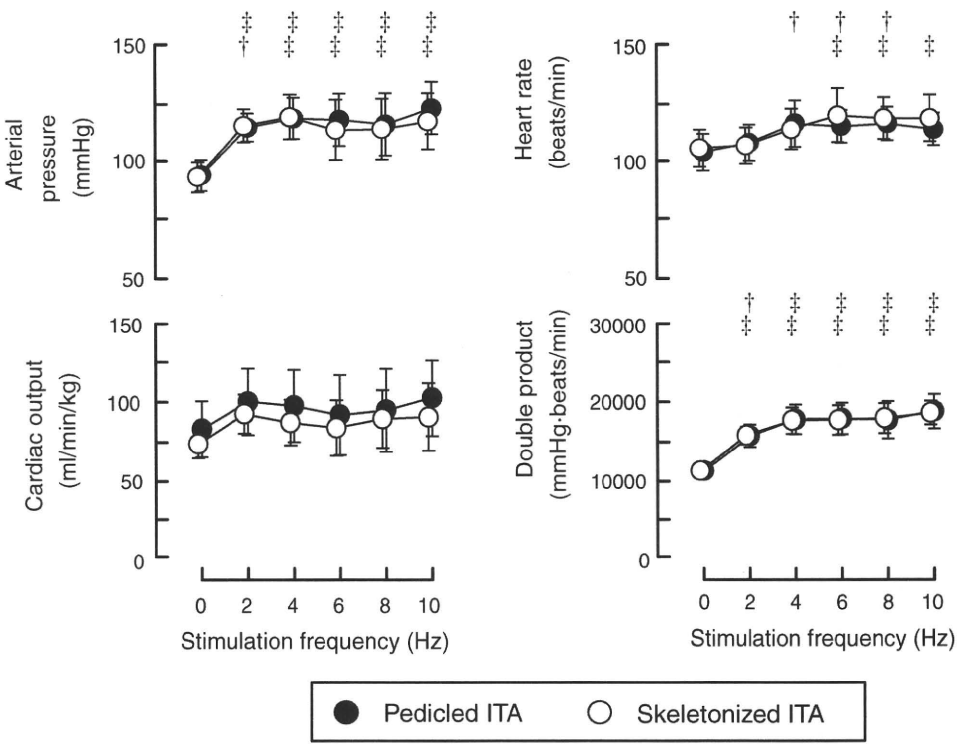

Fig. 2 Changes in mean arterial pressure, cardiac output, heart rate, and double product with pedicled (*closed circle*) and skeletonized (*open circle*) ITAs during sympathetic nerve stimulation. Data are shown as the mean ± SE. $^{\dagger}P < 0.05$ vs. baseline, $^{\ddagger}P < 0.01$ vs. baseline

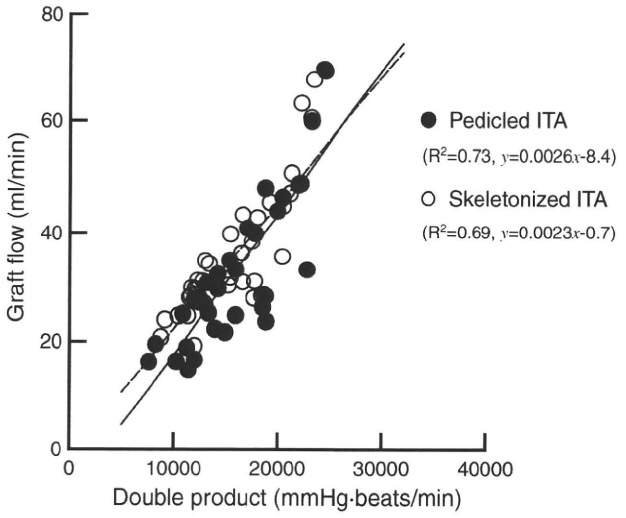

Fig. 3 Scatter plots and regressions between the double product and graft flow with pedicled (*closed circle*, *solid line*) and skeletonized (*open circle*, *dashed line*) ITAs. Regression lines did not differ between the two groups. y Graft flow, x double product

because the use of contrast medium in angiography may have affected the graft flow through its vasodilatative effect on the coronary artery [11].

Another explanation may be the difference in background sympathetic tone. As the skeletonized graft flow was always studied in the later phase of the experiment, when background sympathetic tone and myocardial metabolic demand may be higher, skeletonized graft flow may have been higher for this reason. The presence of similar hemodynamics during the two protocols, however, does not directly support this explanation. The hemodilution seen predominantly in the later phase of the experiment may also have contributed to higher flow through the skeletonized graft under baseline conditions.

The fact that graft flows were similar between the skeletonized and pedicled ITAs during maximal sympathetic excitation indicates that the resistance of the ITA graft was much smaller than that of the native coronary bed, even when the coronary bed was maximally dilated to meet the oxygen demand present with maximal sympathetic stimulation. In other words, both the skeletonized and pedicled ITAs would appear to provide sufficient flow reserve to the LAD area. In contrast, it has been reported that free flow, which may represent the maximal flow capacity of the ITA itself, is greater in the skeletonized ITA than in the pedicled ITA [2, 3]. Despite these previous findings, because the maximally dilated native coronary bed would be the most practical downstream conduit to test the difference between the skeletonized and pedicled ITAs, we believe that the difference in sympathetic innervation does not affect the maximal flow significantly under anastomosed conditions.

In addition to the effects of downstream resistance, local mechanisms would also contribute to the observed difference in flow between the pedicled and skeletonized ITA grafts. Complete sympathetic denervation with the local application of phenol to the skeletonized ITA further increased graft flow (unpublished observation), suggesting that there remains a certain sympathetic innervation in the skeletonized ITA. Even though sympathetic denervation may not be complete after skeletonization, we believe that our skeletonization did not differ greatly from those clinically performed by surgeons. Deja et al. [4] reported that skeletonization increases the reactivity of ITA to norepinephrine in vitro. Their study may support our results. Prior to sympathetic stimulation but under spontaneous sympathetic outflow, the amount of endogenous norepinephrine release to the skeletonized ITA may be relatively smaller than that to the pedicled ITA; as such, the sympathetic vasoconstriction would be negligible in the skeletonized ITA. This may explain the larger graft flow in the skeletonized ITA prior to sympathetic stimulation. Under maximal sympathetic stimulation, however, hyperreactivity to endogenous norepinephrine in the skeletonized ITA may cause the sympathetic vasoconstriction similar to that occurring in the pedicled ITA. This local mechanism may also partly account for why graft flow was comparable between the pedicled and skeletonized ITAs during maximal sympathetic stimulation. Although the results from several pharmacological studies suggest that norepinephrine-induced vasoconstriction does occur in the ITA [12, 13], there have been no reports assessing the tissue norepinephrine concentration of ITA during sympathetic stimulation. Further investigations are necessary to gain an understanding of the difference in norepinephrine reactivity between the pedicled and skeletonized ITAs.

Some publications have reported several advantages of the skeletonized ITA grafts other than the potential increase in graft flow at rest [1, 14]. Firstly, skeletonization lengthens the ITA, thereby providing access to more distal targets in the coronary artery [15]. Second, skeletonization improves blood supply to the sternum (measured by single photon emission computed tomography) [16] compared with pedicled harvesting. Third, skeletonization decreases the incidence of postoperative respiratory dysfunction because of less invasive harvesting (i.e., preserved pleural integrity in skeletonized ITA vs. pleurotomy in pedicled ITA) [17, 18]. Lastly, skeletonization markedly reduces anterior chest pain and dysesthesia 3 months after surgery [19]. In contrast to these advantages, skeletonization has the minor disadvantages of greater technical difficulty, longer harvesting duration, and potential damage to the graft.

Limitations

This study has several limitations. First, because skeletonized graft flow measurements always follow pedicled graft flow measurements in the same dog, the effect of time sequence on graft flows cannot be ruled out. Nevertheless, the similar hemodynamic response to sympathetic stimulation between protocol 1 and 2 (Fig. 2) suggests that the animal conditions did not deteriorate considerably. Second, the perfusion area of LITA was limited to the LAD region. If we had used a much larger perfusion area of LITA, the possible small difference between the pedicled and skeletonized ITAs may have been revealed. Third, a histological comparison between the pedicled and skeletonized ITA was not performed because the pedicled ITA was always skeletonized after the protocol 1, and the tissue samples from the pedicled ITA could not be obtained. Further investigations that include histological comparison are necessary for examining the effect of skeletonization on sympathetic innervations.

Conclusion

Both the pedicled and skeletonized ITA techniques supplied similar, adequate blood flow to the LAD, meeting myocardial oxygen demand during sympathetic excitation. Metabolic demand can override the possible difference in sympathetic vasoconstriction, increasing the flow in both pedicled and skeletonized ITA grafts to a similar extent when they are anastomosed to LAD. The results of this study have an important implication in terms of clinical application. Following anastomosis, graft flow is highly variable and is dependent on myocardial oxygen demand. Because the quality of CABG may be judged based on flow through anastomosed grafts, one has to take into consideration the potential change in flow in response to myocardial oxygen demand.

Acknowledgments This study was supported by Health and Labor Sciences Research Grants (H18-nano-Ippan-003, H19-nano-Ippan-009, H20-katsudo-Shitei-007 and H21-nano-Ippan-005) from the Ministry of Health, Labor and Welfare of Japan, by Grants-in-Aid for Scientific Research (No. 20390462) from the Ministry of Education, Culture, Sports, Science and Technology in Japan and by the Industrial Technology Research Grant Program from New Energy and Industrial Technology Development Organization (NEDO) of Japan.

References

1. Del Campo C (2003) Pedicled or skeletonized? A review of the internal thoracic artery graft. Tex Heart Inst J 30:170–175
2. Castro GP, Dussin LH, Wender OB, Barbosa GV, Saadi EK (2005) Comparative analysis of the flows of left internal thoracic artery grafts dissected in the pedicled versus skeletonized manner for myocardial revascularization surgery. Arq Bras Cardiol 84:261–266
3. Deja MA, Woś S, Gołba KS, Zurek P, Domaradzki W, Bachowski R, Spyt TJ (1999) Intraoperative and laboratory evaluation of skeletonized versus pedicled internal thoracic artery. Ann Thorac Surg 68:2164–2168
4. Deja MA, Gołba KS, Malinowski M, Woś S, Kolowca M, Biernat J, Kajor M, Spyt TJ (2005) Skeletonization of internal thoracic artery affects its innervation and reactivity. Eur J Cardiothorac Surg 28:551–557
5. Wendler O, Tscholl D, Huang Q, Schäfers HJ (1999) Free flow capacity of skeletonized versus pedicled internal thoracic artery grafts in coronary artery bypass grafts. Eur J Cardiothorac Surg 15:247–250
6. Onorati F, Esposito A, Pezzo F, di Virgilio A, Mastroroberto P, Renzulli A (2007) Hospital outcome analysis after different techniques of left internal mammary grafts harvesting. Ann Thorac Surg 84:1912–1919
7. Takami Y, Ina H (2002) Effects of skeletonization on intraoperative flow and anastomosis diameter of internal thoracic arteries in coronary artery bypass grafting. Ann Thorac Surg 73:1441–1445
8. Austen WG, Edwards JE, Frye RL, Gensini GG, Gott VL, Griffith LS, McGoon DC, Murphy ML, Roe BB (1975) A reporting system on patients evaluated for coronary artery disease. Report of the Ad Hoc Committee for Grading of Coronary Artery Disease, Council on Cardiovascular Surgery, American Heart Association. Circulation 51:5–40
9. Kitamura K, Jorgensen CR, Gobel FL, Taylor HL, Wang Y (1972) Hemodynamic correlates of myocardial oxygen consumption during upright exercise. J Appl Physiol 32:516–522
10. Dönmez A, Tufan H, Tutar N, Araz C, Sezgin A, Karadeli E, Torgay A (2005) In vivo and in vitro effects of stellate ganglion blockade on radial and internal mammary arteries. J Cardiothorac Vasc Anesth 19:729–733
11. Baile EM, Paré PD, D'yachkova Y, Carere RG (1999) Effect of contrast media on coronary vascular resistance: contrast-induced coronary vasodilation. Chest 116:1039–1045
12. Evora PR, Pearson PJ, Discigil B, Oeltjen MR, Schaff HV (2002) Pharmacological studies on internal mammary artery bypass grafts. Action of endogenous and exogenous vasodilators and vasoconstrictors. J Cardiovasc Surg (Torino) 43:761–771
13. He GW, Yang CQ, Starr A (1995) Overview of the nature of vasoconstriction in arterial grafts for coronary operations. Ann Thorac Surg 59:676–683
14. Athanasiou T, Crossman MC, Asimakopoulos G, Cherian A, Weerasinghe A, Glenville B, Casula R (2004) Should the internal thoracic artery be skeletonized? Ann Thorac Surg 77:2238–2246
15. Higami T, Yamashita T, Nohara H, Iwahashi K, Shida T, Ogawa K (2001) Early results of coronary grafting using ultrasonically skeletonized internal thoracic arteries. Ann Thorac Surg 71:1224–1228
16. Cohen AJ, Lockman J, Lorberboym M, Bder O, Cohen N, Medalion B, Schachner A (1999) Assessment of sternal vascularity with single photon emission computed tomography after harvesting of the internal thoracic artery. J Thorac Cardiovasc Surg 118:496–502
17. Bonacchi M, Prifti E, Giunti G, Salica A, Frati G, Sani G (2001) Respiratory dysfunction after coronary artery bypass grafting employing bilateral internal mammary arteries: the influence of intact pleura. Eur J Cardiothorac Surg 19:827–833
18. Matsumoto M, Konishi Y, Miwa S, Minakata K (1997) Effect of different methods of internal thoracic artery harvest on pulmonary function. Ann Thorac Surg 63:653–655

19. Boodhwani M, Lam BK, Nathan HJ, Mesana TG, Ruel M, Zeng W, Sellke FW, Rubens FD (2006) Skeletonized internal thoracic artery harvest reduces pain and dysesthesia and improves sternal perfusion after coronary artery bypass surgery: a randomized, double-blind, within-patient comparison. Circulation 114:766–773

Effect of linear ablation on spectral components of atrial fibrillation

Miki Yokokawa, MD,* Aman Chugh, MD,* Magnus Ulfarsson, PhD,† Hiroshi Takaki, MD, PhD,‡ Li Han, PhD,* Kentaro Yoshida, MD,* Masaru Sugimachi, MD, PhD,‡ Fred Morady, MD, Hakan Oral, MD*

*From the *Division of Cardiovascular Medicine, University of Michigan, Ann Arbor, Michigan, †Department of Electrical and Computer Engineering, University of Iceland, Reykjavik, Iceland, and ‡Department of Cardiovascular Dynamics, National Cardiovascular Center Research Institute, Osaka, Japan.*

BACKGROUND Spectral components of atrial fibrillation (AF) other than the dominant frequency (DF) may represent macroreentrant circuits that coexist with higher-frequency sources during AF.

OBJECTIVE The purpose of this study was to determine whether spectral components of AF can be eliminated by targeted linear ablation.

METHODS Antral pulmonary vein isolation (APVI) and linear ablation were performed in 26 patients (age 60 ± 11 years) to eliminate long-standing persistent AF (duration 3 ± 2 years). Spectral analysis of atrial activation at multiple atrial sites was performed during AF, at baseline, after APVI, and immediately before and after liner ablation along the roof of the left atrium, mitral isthmus, and cavotricuspid isthmus. The prevalence and spatial distribution of spectral components of AF were examined before and after each step of ablation.

RESULTS Twelve (46%) of 26 patients had conversion of AF to atrial tachycardia (AT) during ablation. Mean cycle length of AT was 237 ± 25 ms. A spectral component of AF (3.7 ± 1.2 Hz) other than the DF (6.0 ± 0.9 Hz) was present in 74 (43%) of 173 baseline AF periodograms at multiple atrial sites. Following APVI, no difference in the prevalence of spectral components was seen (38% vs 43%, $P = .38$). However, linear ablation resulted in a significant decrease in the prevalence of spectral components (24% vs 43%, $P < .01$), but only when complete conduction block was achieved.

CONCLUSION Elimination of spectral components of AF by targeted linear ablation suggests that spectral components may indicate site-specific ATs that coexist with AF despite a lower frequency than the DF of AF.

KEYWORDS Atrial fibrillation; Atrial tachycardia; Catheter ablation; Spectral analysis

ABBREVIATIONS **AF** = atrial fibrillation; **APVI** = antral pulmonary vein isolation; **AT** = atrial tachycardia; **CFAE** = complex fractionated atrial electrogram; **CS** = coronary sinus; **DF** = dominant frequency; **LA** = left atrium; **PV** = pulmonary vein; **RA** = right atrium

(Heart Rhythm 2010;7:1732–1737)

A study that analyzed the spectral characteristics of atrial fibrillation (AF) suggested that atrial tachycardias (ATs) to which AF converts during radiofrequency ablation may represent organized tachycardias that coexist with AF despite a lower frequency than the dominant frequency (DF) of AF.[1] If this were the case, targeted linear ablation might eliminate the lower-frequency components.

The purpose of this study was to determine whether linear ablation at sites frequently used by ATs eliminates specific spectral components of AF in patients with persistent AF.

Supported in part by a grant from the Leducq Transatlantic Network.
Address reprint requests and correspondence: Dr. Hakan Oral, Cardiovascular Center, SPC 5853, 1500 East Medical Center Drive, Ann Arbor, Michigan 48109-5853. E-mail address: oralh@umich.edu. (Received May 17, 2010; accepted 2010.)

Methods

Study subjects

The study consisted of 26 patients (23 men and 3 women; mean age 60 ± 11 years, range 35–77 years) with persistent AF who underwent radiofrequency catheter ablation. Mean left atrial (LA) diameter was 46 ± 6 mm, and left ventricular ejection fraction was 0.54 ± 0.09. AF was first diagnosed 8 ± 8 years before presentation and was persistent for 3 ± 2 years before ablation (range 1–7 years). Two patients had coronary artery disease. The clinical characteristics of the patients are listed in Table 1. Patients with a prior ablation procedure were excluded from the study.

Electrophysiologic study

The study protocol was approved by the Institutional Review Board. All patients provided informed written consent. Antiarrhythmic drug therapy was discontinued ≥5 half-lives before electrophysiologic study, except for amiodarone, which was discontinued >8 weeks before the proce-

1547-5271/$ -see front matter doi:10.1016/j.hrthm.2010.05.040

Table 1 Patient characteristics

Age (years)	60 ± 11
Gender (male/female)	19/7
Duration of atrial fibrillation (years)	3 ± 2
Left atrial diameter (mm)	46 ± 6
Left ventricular ejection fraction	0.54 ± 0.09
Coronary artery disease (%)	2 (8)

Values are given as mean ± SD.

dure. Electrophysiologic study was performed in the fasting state under conscious sedation using fentanyl and midazolam. Vascular access was obtained through a femoral vein. A decapolar catheter (E-Z Steer CS Decapolar, Biosense Webster, Diamond Bar, CA, USA) was positioned in the coronary sinus (CS). Immediately after the transseptal puncture, systemic anticoagulation was achieved with intravenous heparin, and the activated clotting time was maintained between 300 and 350 seconds throughout the procedure. The pulmonary veins (PVs) were mapped with a decapolar ring catheter (Lasso, Biosense Webster) advanced to the LA. Mapping and ablation were performed using a 3.5-mm open irrigation tip catheter (ThermoCool NaviStar, Biosense Webster). Bipolar electrograms were displayed and recorded at filter settings of 30 to 500 Hz during the procedure (EPMed Systems, West Berlin, NJ, USA). Electrograms were also recorded at 0.5 to 200 Hz for offline spectral analysis.

Catheter navigation and ablation were performed with guidance from an electroanatomic mapping system (CARTO, Biosense Webster). Radiofrequency energy was delivered at a maximum power of 20 to 25 W at a flow rate of 17 mL/min near the PVs, along the posterior wall, and within the CS and at a maximum power of 35 W at a flow rate of 30 mL/min elsewhere in the atria. Maximum temperature was set at 48°C.

Study protocol and ablation strategy

All patients presented to the laboratory in AF, and ablation was performed during AF. First, antral pulmonary vein isolation (APVI) was performed to isolate all PVs and resulted in termination of AF in 1 of 26 patients. Therefore, the study protocol was completed in the remaining 25 patients who remained in AF after APVI. In these 25 patients, linear ablation along the LA roof and mitral isthmus was performed (Figure 1). At the discretion of the operator, complex fractionated atrial electrograms (CFAEs) were targeted in 20 (80%) of 25 patients. CFAE ablation was performed before linear ablation in 12 (60%) of 20 patients and after liner ablation in 8 (40%) of 20 patients. Linear ablation along the cavotricuspid isthmus was performed in 5 patients who had a history of typical atrial flutter. Whenever AF converted to an AT, entrainment and activation mapping were performed to guide ablation of the AT. Sinus rhythm was restored by transthoracic cardioversion in patients who remained in AF after ablation. After sinus rhythm was restored, conduction block across the LA roof, mitral isthmus, and cavotricuspid isthmus lines was assessed.[2–4] If necessary, additional ablation was performed to achieve complete block.

Prior to ablation, all PVs were mapped with a decapolar ring catheter. Electrograms then were recorded for ≥30 seconds at ≥2 different locations (tagged on the map; Figure 1) at each of the following sites: (1) LA roof, (2) mitral isthmus, (3) LA appendage, (4) LA septum, (5) CS, (6) cavotricuspid isthmus, and (7) right atrial (RA) appendage. Caution was exercised to create linear lesions ≥5 mm from the sampling sites. Sampling was performed at baseline, after APVI, (and also after CFAE ablation when applicable), and immediately before and immediately after linear ablation without any CFAE ablation between the two sampling times.

Digital signal processing and data analysis

Electrograms were processed offline in the MatLab environment (MathWorks, Inc., Natick, MA, USA) using custom software as described previously.[1] In brief, first digitized bipolar electrograms sampled for ≥30 seconds at 2,000 Hz underwent preprocessing steps of bandpass filtering at 40 to 250 Hz, rectification, and low-pass filtering at 20 Hz. Then the discrete Fourier transform of the prepro-

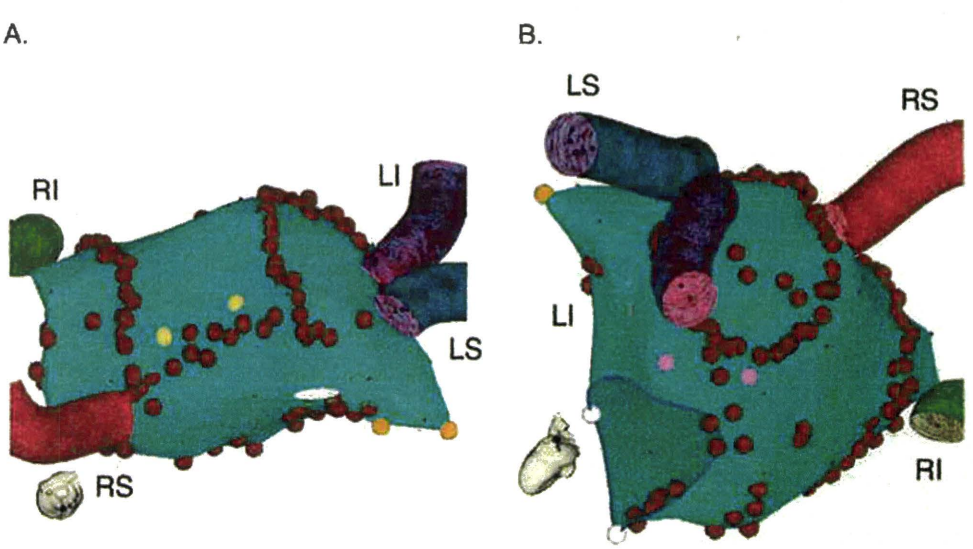

Figure 1 Antral pulmonary vein isolation and linear ablation. Shown is the three-dimensional reconstruction of the left atrium and pulmonary veins during ablation of atrial fibrillation (**A:** craniocaudal projection; **B:** left posterior oblique projection). Electrograms were recorded for ≥30 seconds at ≥2 different positions at each atrial site. *Red tags* indicate ablation sites. *Yellow tags* and *pink tags* indicate sampling sites. LI = left inferior; LS = left superior; RI = right inferior; RS = right superior.

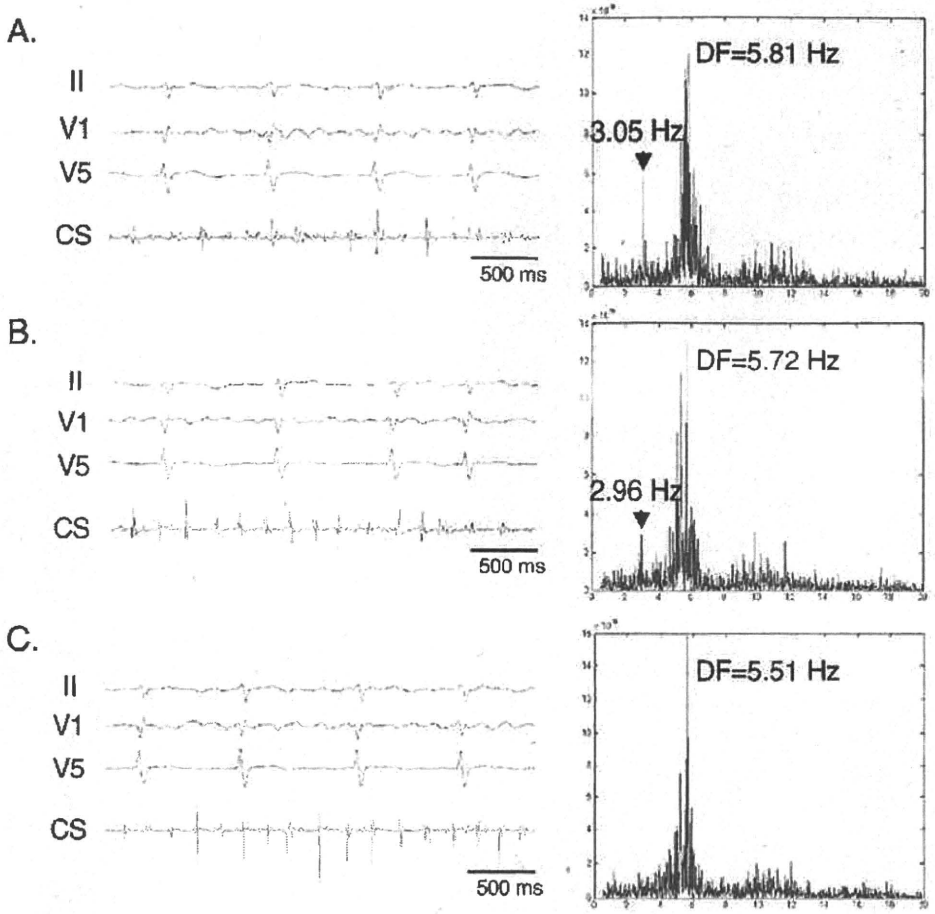

Figure 2 Time- and frequency-domain characteristics of atrial fibrillation (AF) recorded in the coronary sinus (CS). **A:** At baseline, the dominant frequency (DF) of AF was 5.81 Hz, and there was a spectral component with a frequency of 3.05 Hz *(arrow)*. **B:** Antral pulmonary vein isolation (APVI) did not have an effect on the spectral component. **C:** After linear ablation, however, the spectral component was no longer present. Shown are ECG leads II, V_1, and V_5 and bipolar intracardiac electrograms recorded from the CS.

cessed signal was computed using the fast Fourier transformation algorithm to analyze the 0.5- to 80-Hz spectral band. DF was defined as the frequency of the highest peak of the smoothed periodogram in the interval from 0.5 to 20 Hz. The periodogram during AF was systemically analyzed to identify spectral components with peak power ≥20% that of the DF. The spatial distribution of the spectral components of AF and the effect of APVI and linear ablation at specific sites were examined. A site was considered to have a spectral component when a spectral component was identified at any of the sampling sites. When far-field ventricular depolarizations were recorded at the annulus, CS, or appendage, the QRS complexes were subtracted. Electrograms without adequate signal-to-noise ratio were excluded from analysis.

Statistical analysis

Continuous variables, expressed as mean ± SD, were compared using Student's t-test. Sequential continuous variables were compared using one-way analysis of variance with repeated measures. Post hoc comparisons were made with the Scheffe test. Categorical variables were compared using Fisher's exact test. $P < .05$ was considered significant.

Results

DF and spectral components of AF at baseline

At baseline, a spectral component with peak power ≥20% that of the DF was identified at 74 (43%) of 173 sites in 23 of 26 patients (3 ± 2 per patient; Figure 2). The mean frequency of the spectral components was 3.7 ± 1.2 Hz, whereas mean DF at the corresponding sites was 6.0 ± 0.9 Hz ($P < .0001$). There was no significant difference in the spatial distribution of the spectral components among the LA, CS, and RA ($P = .48$; Table 2 and Figure 3).

Antral PV isolation

APVI resulted in complete PV isolation in all patients. AF converted to an AT in 1 (4%) of 26 patients after APVI. APVI resulted in a significant decrease in the DF of AF (5.8 ± 0.9 Hz vs 6.1 ± 0.9 Hz, $P = .03$). There was no significant difference in the prevalence of spectral components before (74/173 sites [43%]) and after APVI (42/112 sites [38%],

Table 2 Effects of APVI and linear ablation on the prevalence of spectral components

	Baseline	After APVI	After linear ablation
All	74/173 (43)	42/112 (38)	27/114 (24)*†
Left atrium	47/104 (45)	24/65 (37)	14/66 (21)*†
Coronary sinus	12/26 (46)	8/19 (42)	4/23 (17)
Right atrium	15/43 (35)	10/28 (36)	9/25 (36)

Percent values are shown in parentheses.
APVI = antral pulmonary vein isolation.
*$P < .01$ compared to baseline; †$P < .05$ compared to immediately before linear ablation.

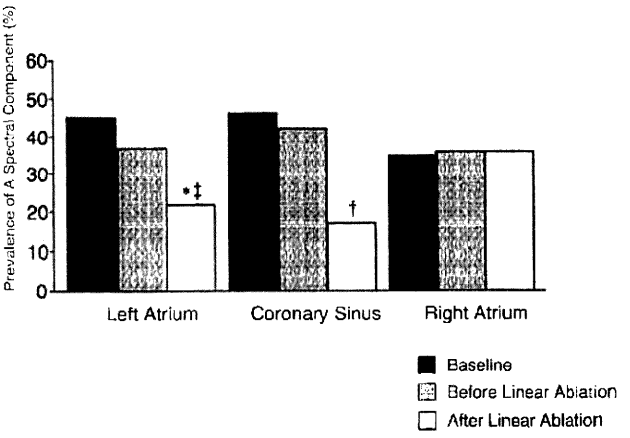

Figure 3 Effect of antral pulmonary vein isolation and linear ablation on the prevalence of spectral components in the left atrium, coronary sinus, and right atrium. *P <.01 and †P = .07 vs compared to baseline; ‡P <.05 compared to immediately before linear ablation.

P = .38; Table 2 and Figure 3). The spatial distribution of the spectral components was also similar before and after APVI (P = .90). There was no significant difference in the mean frequency of the spectral components before and after APVI (3.2 ± 1.2 Hz vs 3.7 ± 1.2 Hz, P = .15).

Ablation of CFAEs did not have a significant effect on the prevalence of spectral components. Among the 12 patients in whom CFAE ablation was performed after APVI but before linear ablation, the prevalence of spectral components was 32% (19/59) after APVI alone and 34% (16/47) after APVI and CFAE ablation (P = .97). Furthermore, the prevalence of spectral components immediately before linear ablation was 34% (16/47) in the 12 patients who had APVI and CFAE ablation before linear ablation and 44% (16/36) in the 8 patients who had CFAE ablation only after linear ablation (P = .33).

Linear ablation

Linear ablation was performed along the LA roof and mitral isthmus in 25 patients and along the cavotricuspid isthmus in 5 patients who remained in AF after APVI. AF converted to an AT in 11 (44%) of 25 patients: after additional linear ablation in 2 patients and after linear and CFAE ablation in 9 patients. Linear ablation was associated with a significant decrease in mean DF in the LA compared to baseline (5.7 ± 0.9 Hz vs 6.1 ± 0.9 Hz, P <.01). There was no significant difference in mean DF after linear ablation compared to the DF after APVI (P = .66). Sinus rhythm was restored by cardioversion in the remaining 14 patients.

Linear ablation resulted in a significant decrease in the prevalence of spectral components with a power ≥20% that of the DF compared to baseline (27/114 sites [24%] vs 74/173 sites [43%], P <.01) and just prior to linear ablation (27/114 sites [24%] vs 42/112 sites [38%], P = .02; Table 2 and Figures 2 and 3). There was a significant decrease in the prevalence of these spectral components after linear ablation at LA sites compared to baseline (14/66 sites [21%] vs 47/104 sites [45%], P <.01) and just prior to linear ablation (14/66 sites [21%] vs 24/65 sites [37%], P <.05). There was a trend toward a decrease in the prevalence of spectral components in the CS (4/23 sites after linear ablation [17%] vs 12/26 sites [46%], P = .07). However, there was no significant change in the prevalence of spectral components at RA sites after linear ablation (9/25 sites [36%] vs 15/43 sites [35%], P = .93).

Linear conduction block and spectral components of AF

Because linear ablation was performed during AF, completeness of conduction block could be assessed only after restoration of sinus rhythm. Complete block was present along the LA roof in 15 (60%) of 25 patients, along the mitral isthmus in 5 (20%) of 25, and along the cavotricuspid isthmus in 2 (40%) of 5 immediately after restoration of sinus rhythm. The spectral components with power ≥20% that of the DF were still present at 12 (55%) of 22 sites with incomplete conduction block and at 0 (0%) of 17 sites with complete conduction block after linear ablation (P <.01). There was no significant change in the mean frequency of spectral components compared to baseline after incomplete linear ablation (3.4 ± 1.0 Hz vs 3.7 ± 1.2 Hz, P = .55).

Prevalence and characteristics of ATs to which AF converts

AF converted to an AT during ablation in 12 (46%) of 26 patients. The mechanism of the ATs was macroreentry in all 12 patients, and their mean cycle length was 237 ± 25 ms (4.3 ± 0.4 Hz). The macroreentrant circuit involved the mitral isthmus in 3 patients, LA roof in 3, interatrial septum in 4, and cavotricuspid isthmus in 2. A spectral component of AF before ablation that matched the frequency of AT was identified at the macroreentrant sites in 6 (50%) of 12 patients (Figure 4). ATs were successfully ablated in all but 4 patients who had pleomorphic ATs. Sinus rhythm was restored by cardioversion in these 4 patients.

DF and termination of AF

At baseline, mean DF was higher among patients who still were in AF after ablation (6.4 ± 0.8 Hz) than among those in whom AF terminated during ablation (5.7 ± 0.9 Hz, P <.0001). Linear ablation was associated with a significant decrease in the DF of AF among patients in whom AF persisted (5.9 ± 0.8 Hz vs 6.4 ± 0.8 Hz, P <.01; Figure 5) and among those in whom AF terminated during ablation (5.3 ± 0.8 Hz vs 5.7 ± 0.9 Hz, P <.01). However, mean DF after linear ablation was still significantly higher when AF persisted than when AF terminated during ablation (5.9 ± 0.8 Hz vs 5.3 ± 0.8 Hz, P <.0001), particularly in the LA appendage (6.1 ± 0.7 Hz vs 5.2 ± 0.9 Hz, P <.01).

Prevalence of spectral components and termination of AF

The prevalence of spectral components of AF at baseline was significantly higher among patients in whom AF persisted than in those in whom AF terminated during ablation

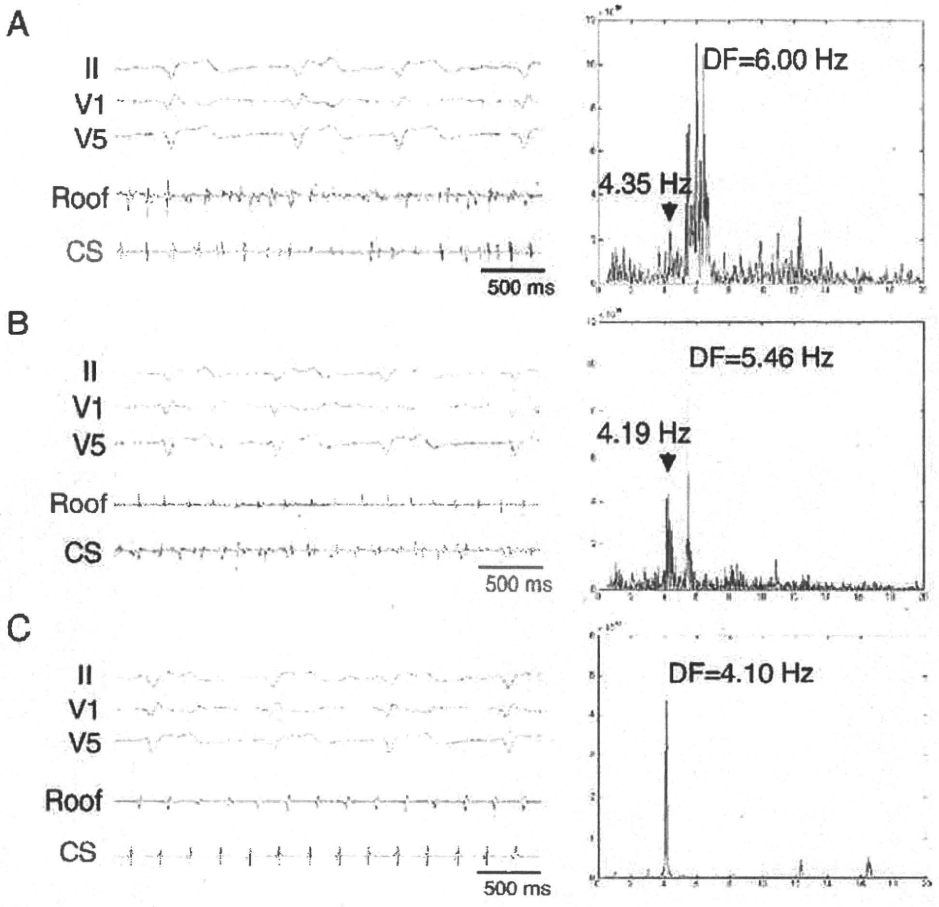

Figure 4 Time- and frequency-domain characteristics of atrial fibrillation (AF) recorded at the left atrial (LA) roof. **A:** At baseline, a spectral component with a frequency of 4.35 Hz was identified *(arrow)*. The simultaneous dominant frequency (DF) was 6 Hz. During linear ablation, AF first became more organized **(B)**, then converted to an atrial tachycardia **(C)**. The frequency of the spectral component during AF at baseline **(A)** and the atrial tachycardia to which AF converted during ablation **(C)** was similar. The flutter circuit used the LA roof and was successfully ablated with a roof line. Shown are ECG leads II, V_1, and V_5 and bipolar intracardiac electrograms recorded from the LA roof and coronary sinus (CS).

(53/92 sites [58%] vs 21/81 sites [26%], $P < .0001$). At baseline, the mean frequency of spectral components was 3.7 ± 1.3 Hz when AF persisted and 3.8 ± 0.9 Hz when AF terminated during ablation ($P = .79$).

Discussion

Major findings

The main findings of this study were as follows. (1) A spectral component with power ≥20% that of the DF was present in 43% of baseline periodograms in patients with persistent AF. (2) Linear ablation, but not APVI, resulted in a significant decrease in the prevalence of these spectral components when complete conduction block was achieved. (3) Spectral components were more prevalent at baseline among patients in whom AF persisted than in those in whom AF terminated during ablation.

Taken together, these findings suggest that spectral components other than the DF may reflect site-specific tachycardias that coexist with AF and can be eliminated by targeted linear ablation. Spectral components of AF appear to reflect contributors of AF perpetuation.

Spectral components of AF

As suggested in a prior study,[1] spectral components of AF may indicate ATs that coexist with AF and that are uncovered after elimination of higher-frequency drivers and fibrillatory conduction by ablation. Because the frequency of the spectral components often matches the frequency of ATs to which AF converts during ablation and because these ATs frequently are macroreentrant circuits that use the roof and mitral isthmus, this study investigated the effects of linear ablation on spectral components.

APVI did not affect the prevalence and frequency of spectral components. CFAE ablation was also performed before (60%) or after linear ablation (40%) in a majority of patients in this study. Similar to APVI, ablation of CFAEs did not have a significant effect on the prevalence of spectral components. However, complete conduction block after linear ablation at these sites led to a significant decrease in the prevalence of spectral components, with no change when conduction block was incomplete. This finding suggests that the spectral components represent underlying macroreentrant circuits eliminated by linear ablation and not simply passive bystander activation or fibrillatory conduction. Furthermore, LA linear ablation had an effect only on the LA spectral components. There was no change in the prevalence of RA spectral components.

An important observation is that APVI resulted in a significant decrease in the DF of AF but had no effect on the frequency of spectral components. Therefore, spectral components likely are not due to passive activation from high-frequency drivers of AF, such as PV tachycardias. If spec-

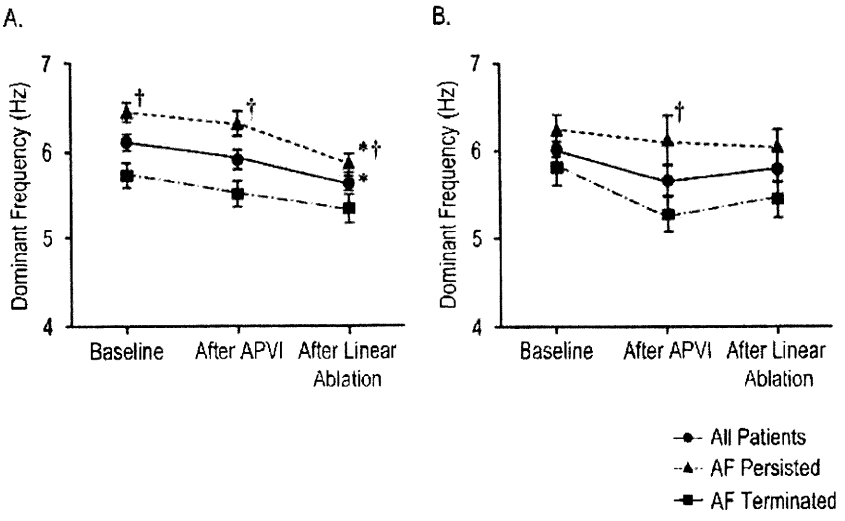

Figure 5 Effect of antral pulmonary vein isolation (APVI) and linear ablation on the dominant frequency of atrial fibrillation (AF) recorded in the left atrium (**A**) and right atrium (**B**) among patients who did and those who did not have termination of AF after ablation. $*P < .01$ compared to baseline; $\dagger P < .01$ among patients who did and those who did not have termination of AF after ablation.

tral components were secondary due to passive activation, a decrease in the DF of AF should have to led to a decrease in the frequency of the spectral components.

Spectral components and termination of AF

Spectral components were more prevalent among patients in whom AF persisted than among those in whom AF terminated during ablation in this study. Because it can be speculated that spectral components represent underlying drivers of AF masked by fibrillatory conduction, a higher prevalence of spectral components may indicate a larger number of contributors to perpetuation of AF and a higher degree of complexity.

This observation suggests that elimination of a few drivers with the highest frequency often may not be sufficient for termination of AF during ablation. The presence and multiplicity of drivers with a lower frequency than the DF of AF may also be important in perpetuating AF.

A prior study demonstrated that linear ablation is necessary to terminate AF in approximately 90% of patients with long-standing persistent AF.[5] Because the roof, mitral isthmus, and cavotricuspid isthmus seldom are the sites with the highest frequency, it is possible that linear ablation exerts its beneficial effect by eliminating underlying secondary or slower drivers of AF.[6] It also is possible that fibrillatory conduction develops out of macroreentrant circuits represented by spectral components during AF.[7]

Study limitations

One limitation of this study is that the prevalence of spectral components may have been underestimated because simultaneous high-density mapping of the LA was not performed. A second limitation is that, due to the effects of ablation and the signal-to-noise ratio, some of the matching electrograms before and after ablation could not be analyzed. However, a sufficient number of electrograms were available for analysis, and the distribution of poor-quality electrograms was random among different sites. Furthermore, there was no difference in the prevalence of spectral components at baseline among sites where samples after linear ablation were and were not available. A third limitation is that because RA ablation was limited to the cavotricuspid isthmus and was performed in only five patients, the effect of RA ablation on prevalence of RA spectral components may have been underestimated.

Clinical implications

The findings of this study suggest that spectral components of AF other than DF may represent underlying ATs likely to play a role in the perpetuation of AF. The ATs that coexist with AF can be eliminated by targeted linear ablation, but only when complete conduction block is achieved, underscoring the importance of assessing conduction block once sinus rhythm has been restored.

Whether spectral components can be identified in real time and used to guide linear ablation during catheter ablation of AF remains to be determined in future studies.

References

1. Yoshida K, Chugh A, Ulfarsson M, et al. Relationship between the spectral characteristics of atrial fibrillation and atrial tachycardias that occur after catheter ablation of atrial fibrillation. Heart Rhythm 2009;6:11–17.
2. Hocini M, Jais P, Sanders P, et al. Techniques, evaluation, and consequences of linear block at the left atrial roof in paroxysmal atrial fibrillation: a prospective randomized study. Circulation 2005;112:3688–3696.
3. Jais P, Hocini M, Hsu LF, et al. Technique and results of linear ablation at the mitral isthmus. Circulation 2004;110:2996–3002.
4. Chugh A, Oral H, Good E, et al. Catheter ablation of atypical atrial flutter and atrial tachycardia within the coronary sinus after left atrial ablation for atrial fibrillation. J Am Coll Cardiol 2005;46:83–91.
5. Haissaguerre M, Hocini M, Sanders P, et al. Catheter ablation of long-lasting persistent atrial fibrillation: clinical outcome and mechanisms of subsequent arrhythmias. J Cardiovasc Electrophysiol 2005;16:1138–1147.
6. Sanders P, Berenfeld O, Hocini M, et al. Spectral analysis identifies sites of high-frequency activity maintaining atrial fibrillation in humans. Circulation 2005;112:789–797.
7. Sahadevan J, Ryu K, Peltz L, et al. Epicardial mapping of chronic atrial fibrillation in patients: preliminary observations. Circulation 2004;110:3293–3299.

The Effect of Donepezil Treatment on Cardiovascular Mortality

K Sato[1], R Urbano[2,3], C Yu[4], F Yamasaki[5], T Sato[6], J Jordan[7], D Robertson[1] and A Diedrich[1,8]

The acetylcholinesterase inhibitor donepezil hydrochloride improves cognitive function in patients with Alzheimer's disease and vascular dementia. Given acetylcholine's important actions on the heart, we undertook a retrospective cohort investigation to assess whether donepezil usage affects cardiovascular mortality. In patients treated with donepezil, hazard ratios for total and cardiovascular mortality were 0.68 ($P = 0.045$, 95% confidence interval 0.46–0.99) and 0.54 ($P = 0.042$, 95% confidence interval 0.30–0.98), respectively. The apparent survival benefit in donepezil-treated patients should not be overinterpreted. Prospective clinical trials are warranted.

The acetylcholinesterase inhibitor donepezil hydrochloride improves cognitive function in patients with Alzheimer's disease and vascular dementia.[1,2] However, this agent also increases the availability of acetylcholine in peripheral tissues, including the heart, where it augments vagal influences on sinus node and cardiac conduction systems. Both sinus node function and conduction deteriorate with age.[3] Aging-associated changes in sinus node function may be related to calcium channel ($Ca_V1.2$) downregulation.[4] A reduction in the levels of connexin-43 expression (which is essential for electrical cell-to-cell stimulation) has been implicated in aging-associated deterioration of the conduction system.[5] Therefore, the elderly and very elderly are at particularly high risk for potentially life-threatening dysfunctions of the sinus node or conduction system. Augmented availability of acetylcholine in the heart through acetylcholinesterase inhibition could conceivably exacerbate the risk of bradycardia in this population. On the other hand, augmented acetylcholine could be beneficial, given the poor cardiovascular outcome in patients with diminished cardiac vagal activity.[6,7] Indeed, acetylcholinesterase inhibition appears to reduce overall mortality in patients with moderate to severe Alzheimer's disease[8] and Parkinson's disease–related dementia.[9] We conducted a retrospective cohort investigation to assess whether donepezil usage affects cardiovascular mortality in patients with Alzheimer's disease or vascular dementia.

RESULTS

We identified 1,004 patients with Alzheimer's disease and vascular dementia out of a total of 1,736 admissions. Donepezil was prescribed for 85 patients at the time of their discharge. Of those, 76 fulfilled all our inclusion and exclusion criteria. Of the 915 patients who did not receive donepezil, we randomly selected 80 patients matched for age, sex, and race to serve as the control group (**Table 1**). The majority of the patients enrolled had Alzheimer's disease. The main reasons for hospital admissions were respiratory symptoms (28%) in donepezil-treated patients and orthopedic (15%) and cardiac causes (15%) in untreated patients.

Over a mean follow-up period of 29 ± 17 months in donepezil-treated patients and 28 ± 25 months in untreated patients, we identified 115 fatal events. Of these, 88 were available in the medical records and were successfully matched to the Tennessee death-certificate database. In 27 patients, fatal events were determined solely from this database. Fatal cardiovascular events occurred in 36 donepezil-treated and 18 untreated patients ($P < 0.01$). Cox proportional hazard regression analysis showed that, relative to the untreated group, donepezil-treated patients had lower total mortality risk and also lower cardiovascular mortality risk (after adjusting for potential confounders such as vascular dementia, age, sex, and ethnicity) (**Table 2**). Additionally, Kaplan–Meier survival analysis showed better overall and cardiovascular survival in donepezil-treated patients in the first 3–4 years of follow-up (**Figure 1**). The intergroup difference disappeared after 4–5 years, probably because of the small number of surviving patients.

[1]Department of Medicine, Division of Clinical Pharmacology, Autonomic Dysfunction Center, Vanderbilt University School of Medicine, Nashville, Tennessee, USA; [2]Vanderbilt Kennedy Center, Vanderbilt University, Nashville, Tennessee, USA; [3]Department of Pediatrics, Vanderbilt University, Nashville, Tennessee, USA; [4]Department of Biostatistics, Vanderbilt University, Nashville, Tennessee, USA; [5]Department of Clinical Laboratory, Kochi Medical School, Nankoku, Japan; [6]Department of Cardiovascular Control, Kochi Medical School, Nankoku, Japan; [7]Institute of Clinical Pharmacology, Hannover Medical School, Hannover, Germany; [8]Department of Biomedical Engineering, Vanderbilt University School of Engineering, Nashville, Tennessee, USA. Correspondence: A Diedrich (andre.diedrich@vanderbilt.edu)

Received 5 March 2010; accepted 23 April 2010; advance online publication 21 July 2010. doi:10.1038/clpt.2010.98

Table 1 Characteristics of the patient population studied

Characteristic	DPZ$^+$ (%) $n = 76$	DPZ$^-$ (%) $n = 80$
Follow-up time (months)[a]	29 ± 17	28 ± 25
Age[a]	80 ± 8	81 ± 8
Sex		
Female	51 (67.1)	54 (67.5)
Male	29 (38.2)	26 (32.5)
Race		
White	63 (82.9)	56 (70)
Nonwhite	17 (22.4)	24 (30)
Diagnosis		
Alzheimer's disease	67 (88.2)	64 (80)
Vascular dementia	9 (11.8)	16 (20)
Chief complaint at time of admission		
Orthopedic	13 (17.1)	12 (15)
Metabolic or nutritional	7 (9.2)	8 (10)
Cerebrovascular event	2 (2.6)	5 (6.3)
Other central nervous system disease	5 (6.6)	5 (6.3)
Cardiac event	14 (18.4)	12 (15)
Respiratory	21 (27.6)	10 (12.5)
GI tract	5 (6.6)	8 (10)

DPZ, donepezil; DPZ$^+$, those who received donepezil medication; DPZ$^-$, those who did not receive donepezil medication; GI, gastrointestinal.

[a]Values are expressed as means ± SDs.

Table 2 Multivariate analysis of hazard ratios for fatal cardiovascular events and all fatal events

	Fatal CV events		All fatal events	
	Hazard ratio (95% CI)	*P* value	Hazard ratio (95% CI)	*P* value
Donepezil medication	0.54 (0.30–0.98)	0.042	0.68 (0.46–0.99)	0.045
Vascular dementia	1.43 (0.69–2.99)	0.338	1.35 (0.82–2.21)	0.234
Age	1.03 (0.99–1.07)	0.095	1.02 (0.99–1.04)	0.151
Male	1.83 (1.03–3.23)	0.038	1.43 (0.97–2.12)	0.071
Nonwhite	1.40 (0.78–2.53)	0.261	1.30 (0.86–1.97)	0.212

CI, confidence interval; CV, cardiovascular.

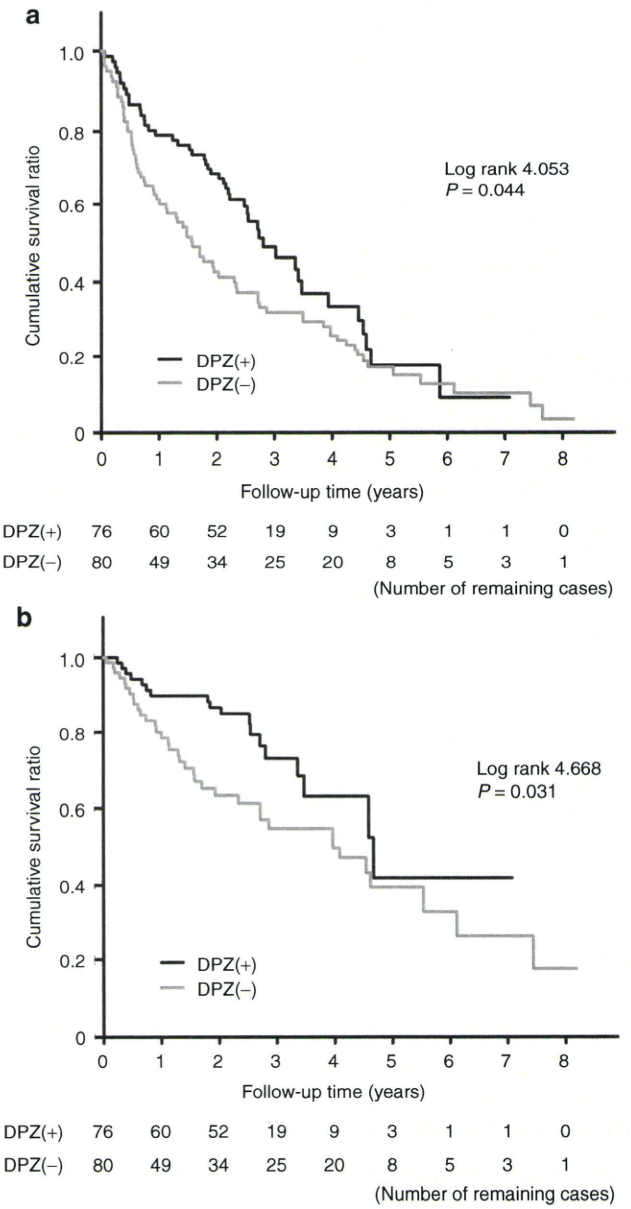

Figure 1 Kaplan–Meier survival curves for (**a**) all fatal events and (**b**) cardiovascular deaths. DPZ, donepezil.

DISCUSSION

Given donepezil's mechanism of action and the high risk for sinus node dysfunction or cardiac conduction impairment in patients receiving the drug, we were concerned that there could be an increase in fatal cardiovascular events in donepezil-treated patients. Instead, our retrospective analysis showed better cardiovascular and overall survival in donepezil-treated patients. Our study has several important limitations and must be interpreted with caution. First, the numbers of patients, both donepezil-treated and untreated, were relatively low. Second, although both groups were carefully matched, a bias such as physicians' decisions on discharge prescriptions could not be eliminated because all the data were retrospectively collected from hospital discharge summaries. Finally, although recent clinical studies demonstrated that donepezil is well tolerated,[2] we have no information concerning medication compliance in our study. Despite these limitations, we believe that our analysis contains clinically relevant information that deserves to be addressed in prospective studies.

Theoretically, donepezil could affect the functioning of the sinus node and cardiac conduction systems through central nervous and peripheral mechanisms. Donepezil has previously been shown to raise brain acetylcholine availability.[10] Central cholinergic stimulation could raise blood pressure through the release of vasopressin[11] and the activation of the sympathoadrenal system.[12] Baroreflex-mediated bradycardia could occur. More likely, acetylcholinesterase inhibition could induce bradycardia through actions on cardiac muscarinic

receptors, as has been shown in rats[11] and in human subjects.[13] However, whether or not donepezil raises heart rate variability, which is strongly influenced by vagal influences on the sinus node, is controversial.[14,15] Previous studies suggested that vagal heart rate control may be impaired in patients with Alzheimer's disease.[16,17] It is possible that such impairment in vagal function could have decreased the likelihood of life-threatening bradycardia in the patients in our study.

Potentially favorable prognostic influences of donepezil may not be confined solely to improvement in cognitive function.[18,19] For instance, tacrine, another cholinesterase inhibitor, did not alter life expectancy in spite of beneficial actions on cognitive and global function.[20] It is possible that augmented vagal function contributes to the survival benefit seen with donepezil. For example, chronic electrical stimulation of the vagus nerve improved long-term survival in rats with congestive heart failure after a large myocardial infarction.[21] Recent studies suggest that acetylcholine from vagal stimulation protects cardiomyocytes from acute hypoxia and ischemia, in part through hypoxia-inducible factor-1α.[22] Moreover, the antiarrhythmia effect of vagal stimulation was accompanied by preservation of phosphorylated connexin-43 protein.[23] Cholinesterase inhibition reduced the levels of thrombomodulin and β-thromboglobulin, which are markers of endothelial and platelet activation, respectively.[24] Finally, donepezil might have a role in direct stimulation of acetylcholine synthesis in cardiomyocytes through mechanisms other than acetylcholinesterase inhibition.[25]

In conclusion, our retrospective cohort study showed that donepezil was associated with reduced cardiovascular mortality in patients with Alzheimer's disease or vascular dementia. Given the limitations of our study, the apparent survival benefit in donepezil-treated patients should not be overinterpreted. However, our observations, as well as data from previous studies suggesting that improved survival is associated with acetylcholinesterase inhibition,[8,26–28] should be scrutinized in mechanistic studies and in larger clinical trials. In particular, we suggest investigating in greater detail the action of donepezil on the cardiovascular system in patients with Alzheimer's disease or vascular dementia. Prospective studies for a duration of several years may be required to gauge the overall risks and benefits of donepezil treatment in this vulnerable population.

Table 3 Outcomes in patients who received donepezil treatment and in those who did not

	DPZ$^+$ (%)	DPZ$^-$ (%)
Survivors	31 (40.8)*	10 (12.5)
Hospital admissions for cardiac events	10 (13.2)	17 (21.3)
Fatal CV events	18 (23.7)*	36 (45.0)
Ischemic heart disease	9 (11.8)	16 (20)
Other heart disease	5 (6.6)	12 (15)
Cerebrovascular diseases	8 (10.5)	4 (5)
Fatal non-CV events	27 (35.5)	34 (43.0)
Neoplasm	2 (2.6)*	14 (17.5)
Malignant solid neoplasm	2 (2.6)	5 (6.3)
Malignant, hematology, and lymph system	0 (0)	3 (3.8)
Malignant unknown neoplasm	0 (0)	6 (7.5)
Metabolic or nutrition	1 (1.3)	4 (5)
Diabetes mellitus	1 (1.3)	1 (1.3)
Lipid disorder	0 (0)	1 (1.3)
Volume depletion	0 (0)	2 (2.5)
Central nervous system	19 (25)*	7 (8.8)
Parkinson's disease	1 (1.3)	0 (0)
Alzheimer's disease	13 (17.1)	5 (6.3)
Unspecified dementia	4 (5.3)	2 (2.5)
Encephalopathy	1 (1.3)	0 (0)
Respiratory system	4 (5.3)	4 (5.0)
Pneumonia	2 (2.6)	3 (3.8)
Other chronic lower respiratory disease	2 (2.6)	0 (0)
Chronic obstructive pulmonary disease	0 (0)	1 (1.3)
Digestive system	0 (0)	4 (5)
Liver disease	0 (0)	2 (2.5)
GI bleeding	0 (0)	1 (1.3)
Cardiac disease	0 (0)	1 (1.3)
Renal system	1 (1.3)	0 (0)
Urinary tract infection	1 (1.3)	0 (0)
Other	0 (0)	1 (1.3)
Complications of medical and surgical care	0 (0)	1 (1.3)

CV, cardiovascular; DPZ, donepezil; DPZ$^+$, those who received donepezil medication; DPZ$^-$, those who did not receive donepezil medication; GI, gastrointestinal.

*$P < 0.01$ for comparisons between the DPZ$^+$ and DPZ$^-$ groups.

METHODS

The institutional review board of Vanderbilt University and the Tennessee Department of Health approved the study protocol.

Data source. We retrospectively obtained data from the Hospital Discharge Data System database of Tennessee, the Vanderbilt Hospital medical record database (StarPanel), and the Tennessee death-certificate database (Tennessee Department of Health Death Data System Manual 2004, Bureau of Health Informatics, Office of Health Statistics). To protect the privacy of the subjects, we removed all traceable, person-specific identifying information from the data set created by linking subjects across the three data sources. Each subject was assigned an anonymous, coded study number.

Patient selection. We included patients with Alzheimer's disease or vascular dementia admitted to Vanderbilt Hospital between 1 January 1997 and 31 December 2003. The clinical diagnosis of probable Alzheimer's disease or vascular dementia was determined by the attending physicians on the basis of the complete medical history, neurological examination, blood chemistry, and computed tomography of the brain. We excluded patients who had a follow-up period of <14 days. The patients had to be Tennessee residents because we relied on the state's death-certificate database. We identified donepezil-treated patients and compared their outcomes with those of randomly selected patients, matched for age, sex, and ethnicity, who had not been treated with donepezil.

Patient characteristics and outcomes. Via the Vanderbilt Medical Center record database (StarPanel), we acquired information on patients' age, sex, ethnicity, residence, dementia diagnosis, chief complaint at admission, past medical history, prognosis, cardiovascular events, and fatal events. Dates and causes of death were identified from the Tennessee

death-certificate database (Tennessee Department of Health Death Data System Manual 2004, Bureau of Health Informatics, Office of Health Statistics) up to 31 December 2005. Patients who survived up to the time of discharge from the hospital and whose names were not found in the death-certificate database up to the cutoff date were considered to be alive as of that date. We use the major code of the Tennessee death-certificate database for demographic description and analysis of data for patients who had fatal events. The causes of death were organized in subclasses as shown in Table 3. The primary end point was a fatal cardiovascular event. The secondary end point was occurrence of any fatal event. Cardiac events experienced by the patients, including acute coronary syndrome or decompensated heart failure at the time of admission to Vanderbilt Hospital, were investigated. Furthermore, any cardiovascular event for which patients were admitted to the Vanderbilt cardiac unit during the follow-up period was also investigated.

Statistical analysis. Demographic distributions and clinical characteristics were determined for subjects who were prescribed donepezil (DPZ^+ group) and for those who were not (DPZ^- group). Data are presented as mean ± SD for continuous variables and as frequencies for categorical variables. Comparisons between the two groups were performed using Mann–Whitney *U*-tests. The Pearson χ^2-test was used for categorical variables. Overall patient survival was analyzed using a Cox proportional hazards model to control for covariates. Cox proportional hazards regression models were applied to compare survival rates in the DPZ^+ and DPZ^- patients at the time of discharge from the hospital. The models were adjusted for the effect of independent mortality risk factors including vascular dementia, age, sex, and race. Kaplan–Meier survival curves were constructed to assess the probability of survival free from all fatal events and cardiovascular fatal events. The differences were tested using the log-rank test. A two-tailed P value <0.05 was considered statistically significant. All statistical analyses were performed using SPSS 16.0 (SPSS, Chicago, IL).

ACKNOWLEDGMENTS

Vanderbilt CTSA grant 1 UL1 RR024975 from the National Center for Research Resources/National Institutes of Health (NIH) and a Program Project Grant from the NIH (5P01 HL56693) supported this research. We thank the Tennessee Department of Health for their support. Hospital discharge data from the Tennessee Hospital Discharge Data System and vital statistics data sets were provided by the Tennessee Department of Health, Office of Health Statistics (Nashville, TN).

CONFLICT OF INTEREST

The authors declared no conflict of interest.

1. Feldman, H., Gauthier, S., Hecker, J., Vellas, B., Subbiah, P. & Whalen, E. A 24-week, randomized, double-blind study of donepezil in moderate to severe Alzheimer's disease. *Neurology* **57**, 613–620 (2001).
2. Black, S. *et al.* Efficacy and tolerability of donepezil in vascular dementia: positive results of a 24-week, multicenter, international, randomized, placebo-controlled clinical trial. *Stroke.* **34**, 2323–2330 (2003).
3. Kistler, P.M. *et al.* Electrophysiologic and electroanatomic changes in the human atrium associated with age. *J. Am. Coll. Cardiol.* **44**, 109–116 (2004).
4. Jones, S.A., Boyett, M.R. & Lancaster, M.K. Declining into failure: the age-dependent loss of the L-type calcium channel within the sinoatrial node. *Circulation* **115**, 1183–1190 (2007).
5. Jones, S.A., Lancaster, M.K. & Boyett, M.R. Ageing-related changes of connexins and conduction within the sinoatrial node. *J. Physiol. (Lond.)* **560**, 429–437 (2004).
6. La Rovere, M.T. *et al.* Baroreflex sensitivity and heart rate variability in the identification of patients at risk for life-threatening arrhythmias: implications for clinical trials. *Circulation* **103**, 2072–2077 (2001).
7. Lechat, P. *et al.* Heart rate and cardiac rhythm relationships with bisoprolol benefit in chronic heart failure in CIBIS II Trial. *Circulation* **103**, 1428–1433 (2001).
8. Winblad, B. *et al.* A 1-year, randomized, placebo-controlled study of donepezil in patients with mild to moderate AD. *Neurology* **57**, 489–495 (2001).
9. Moretti, R., Torre, P., Vilotti, C., Antonello, R.M. & Pizzolato, G. Rivastigmine and Parkinson dementia complex. *Expert Opin. Pharmacother.* **8**, 817–829 (2007).
10. Kosasa, T., Kuriya, Y., Matsui, K. & Yamanishi, Y. Inhibitory effects of donepezil hydrochloride (E2020) on cholinesterase activity in brain and peripheral tissues of young and aged rats. *Eur. J. Pharmacol.* **386**, 7–13 (1999).
11. Lazartigues, E. *et al.* Pressor and bradycardic effects of tacrine and other acetylcholinesterase inhibitors in the rat. *Eur. J. Pharmacol.* **361**, 61–71 (1998).
12. Savci, V., Gürün, M.S., Cavun, S. & Ulus, I.H. Cardiovascular effects of centrally injected tetrahydroaminoacridine in conscious normotensive rats. *Eur. J. Pharmacol.* **346**, 35–41 (1998).
13. Bordier, P. *et al.* Cardiovascular effects and risk of syncope related to donepezil in patients with Alzheimer's disease. *CNS Drugs* **20**, 411–417 (2006).
14. McLaren, A.T., Allen, J., Murray, A., Ballard, C.G. & Kenny, R.A. Cardiovascular effects of donepezil in patients with dementia. *Dement. Geriatr. Cogn. Disord.* **15**, 183–188 (2003).
15. Masuda, Y. & Kawamura, A. Acetylcholinesterase inhibitor (donepezil hydrochloride) reduces heart rate variability. *J. Cardiovasc. Pharmacol.* **41** (suppl 1), S67–S71 (2003).
16. Aharon-Peretz, J., Harel, T., Revach, M. & Ben-Haim, S.A. Increased sympathetic and decreased parasympathetic cardiac innervation in patients with Alzheimer's disease. *Arch. Neurol.* **49**, 919–922 (1992).
17. Wang, S.J. *et al.* Cardiovascular autonomic functions in Alzheimer's disease. *Age Ageing* **23**, 400–404 (1994).
18. Passmore, A.P., Bayer, A.J. & Steinhagen-Thiessen, E. Cognitive, global, and functional benefits of donepezil in Alzheimer's disease and vascular dementia: results from large-scale clinical trials. *J. Neurol. Sci.* **229–230**, 141–146 (2005).
19. Black, S.E. *et al.* Donepezil preserves cognition and global function in patients with severe Alzheimer disease. *Neurology* **69**, 459–469 (2007).
20. Wallin, A.K., Gustafson, L., Sjögren, M., Wattmo, C. & Minthon, L. Five-year outcome of cholinergic treatment of Alzheimer's disease: early response predicts prolonged time until nursing home placement, but does not alter life expectancy. *Dement. Geriatr. Cogn. Disord.* **18**, 197–206 (2004).
21. Li, M., Zheng, C., Sato, T., Kawada, T., Sugimachi, M. & Sunagawa, K. Vagal nerve stimulation markedly improves long-term survival after chronic heart failure in rats. *Circulation* **109**, 120–124 (2004).
22. Kakinuma, Y. *et al.* Acetylcholine from vagal stimulation protects cardiomyocytes against ischemia and hypoxia involving additive non-hypoxic induction of HIF-1α. *FEBS Lett.* **579**, 2111–2118 (2005).
23. Ando, M. *et al.* Efferent vagal nerve stimulation protects heart against ischemia-induced arrhythmias by preserving connexin43 protein. *Circulation* **112**, 164–170 (2005).
24. Borroni, B. *et al.* Cholinesterase inhibitors exert a protective effect on endothelial damage in Alzheimer disease patients. *J. Neurol. Sci.* **229–230**, 211–213 (2005).
25. Kakinuma, Y., Akiyama, T. & Sato, T. Cholinoceptive and cholinergic properties of cardiomyocytes involving an amplification mechanism for vagal efferent effects in sparsely innervated ventricular myocardium. *FEBS J.* **276**, 5111–5125 (2009).
26. Ott, B.R. & Lapane, K.L. Tacrine therapy is associated with reduced mortality in nursing home residents with dementia. *J. Am. Geriatr. Soc.* **50**, 35–40 (2002).
27. Gasper, M.C., Ott, B.R. & Lapane, K.L. Is donepezil therapy associated with reduced mortality in nursing home residents with dementia? *Am. J. Geriatr. Pharmacother.* **3**, 1–7 (2005).
28. López-Pousa, S. *et al.* Comparative analysis of mortality in patients with Alzheimer's disease treated with donepezil or galantamine. *Age Ageing* **35**, 365–371 (2006).

In the Spotlight: BioInstrumentation

Ken-ichi Yamakoshi, *Member, IEEE*

I. Introduction

OVER recent decades a very large number of studies have been vigorously carried out to develop invasive and non-invasive physiological measurement bioinstrumentation, for use in areas such as basic and clinical medicine, healthcare and welfare science, sports science, and others. Noninvasive measurement is generally considered to be the most desirable approach for practical use, but in addition there is a significant increasing need to monitor physiological variables in a manner that allows the subject to be unconstrained, which can be achieved by the so-called ambulatory or wearable monitoring techniques. This means that biological sensors and/or miniaturized measuring units are to be carried by the subject or are to be embedded in his/her clothes. The development of such monitoring approaches through modern technological advances has progressed remarkably, and this review briefly introduces several areas where such recent advances have been made.

II. Ambulatory/Wearable Physiological Monitoring

As is well recognised, the first attempts to develop a portable ECG device with radio telemetry, called "*Radioelectrocardiography*" [1], and then with tape recording [2] were reported by N. J. Holter. Refinements of such systems are now commercially available and widely used in clinics as the Holter ECG recorder [see [3]]. Following Holter's epoch-making initiative, numerous research studies have been carried out aiming to monitor a wide range of physiological variables during ambulatory use. In particular, a portable sphygmomanometer, the "ambulatory blood pressure monitor (ABPM)" [4], [5], which is based on the auscultation and/or cuff-oscillometric method [6], has been one successful example akin to the Holter ECG recorder, and these two are now widely used in clinical medicine as key devices. Also, modern micro-electronics and mechanical technologies have enabled us to produce more compact and convenient devices for home use.

Fig. 1 shows the basic construction of a typical ambulatory/wearable monitoring system, consisting of a biological sensing unit (BSU), a portable measuring unit (PMU) for signal processing and data storage, and a data reproducing and display unit (DRU), which is usually a conventional personal computer (PC). The BSU and the PMU are carried by the subject, and in the BSU are either conventional biological sensors/electrodes or sensing devices embedded into the subject's clothes. For signal processing and data storage in the PMU, a microcomputer-based system is usually adopted at present to make it more compact and convenient to operate. Over the last decade advances in information and communication technologies have led to the use of wireless communications between BSU and PMU and between PMU and DRU.

A selection of recent attempts at physiological monitoring relating in particular to cardio-pulmonary, human activity and biochemical information are now briefly described.

A. Cardio-Pulmonary Monitoring

Due to the importance of evaluating cardiovascular and pulmonary function there have been many attempts over the past several decades to develop appropriate ambulatory/wearable physiological measurement systems. These have been based on key physiological variables, including the ECG, blood pressure (BP) and respiration.

Considerable improvements as compared with the initial Holter ECG recorder have been made in terms of miniaturization and data storage in the PMU and regarding data communications. In addition, much effort has been given to improving the design and fabrication of ECG electrodes. Wet-gelled spot

Manuscript received September 08, 2010; accepted September 24, 2010. Date of publication October 28, 2010; date of current version December 03, 2010.

K. Yamakoshi is with the Graduate School of Natural Science & Technology, Kanazawa University, Kakuma, Kanazawa 920-1192, Japan (e-mail: yamakosi@t.kanazawa-u.ac.jp).

Digital Object Identifier 10.1109/RBME.2010.2089616